Published OnlineFirst July 18, 2013; DOI: 10.1158/0008-5472.CAN-12-3186

Priority Report

Cancer Research

Mammary Tumor Formation and Metastasis Evoked by a HER2 Splice Variant

Abdullah Alajati[1], Nina Sausgruber[1], Nicola Aceto[1], Stephan Duss[1], Sophie Sarret[1], Hans Voshol[2], Debora Bonenfant[2], and Mohamed Bentires-Alj[1]

Abstract

The *HER2* gene is amplified and overexpressed in approximately 20% of invasive breast cancers where it is associated with metastasis and poor prognosis. Here, we describe a constitutively active splice variant of HER2 (Delta-HER2) in human mammary epithelial cells that evokes aggressive breast cancer phenotypes. Delta-HER2 overexpression in mammary epithelial cells was sufficient to reduce apoptosis, increase proliferation, and induce expression of mesenchymal markers, features that were associated with greater invasive potential in three-dimensional cultures *in vitro* and more aggressive tumorigenicity and metastasis *in vivo*. In contrast, overexpression of wild-type HER2 was insufficient at evoking such effects. Unbiased protein–tyrosine phosphorylation profiling in Delta-HER2–expressing cells revealed increased phosphorylation of several signaling proteins not previously known to be controlled by the HER2 pathway. Furthermore, microarray expression analysis revealed activation of genes known to be highly expressed in ER-negative, high-grade, and metastatic primary breast tumors. Together, our results provide mechanistic insights into the activity of a highly pathogenic splice variant of HER2. *Cancer Res; 73(17); 5320–7. ©2013 AACR.*

Introduction

Each year, breast cancer is diagnosed in over one million women worldwide. Although overall survival rates for breast cancer have improved significantly over the decades, more than 450,000 lives are still lost annually to this disease (1). Improved understanding of how breast cancer arises and progresses is urgently needed. The EGF receptor 2 gene (*ERBB2* or *HER2*) is amplified and overexpressed in approximately 20% of invasive breast cancers and is associated with metastasis and a poor prognosis (2). Trastuzumab is a U.S. Food and Drug Administration-approved humanized antibody targeting HER2 and, in the adjuvant setting, is used together with chemotherapy to treat HER2-overexpressing breast cancers. However, 70% of treated patients do not respond to trastuzumab and 66% to 88% of initial responders become resistant to the drug (3). Despite numerous research and clinical studies, attempts to interfere with the action of the HER2 receptor alone have failed to yield a widely effective treatment. Therefore, it is important to identify proteins within this pathway that could be targeted in combination with trastuzumab or where trastuzumab fails.

p95-HER2, a truncated form of HER2 lacking the extracellular domain, is expressed in human breast tumors, where it activates multiple signaling pathways based on its ability to form homodimers (4). Notably, p95-HER2 evokes mammary tumor growth and metastases in preclinical models (5). Similarly, expression of a splice variant of HER2 lacking exon 16, named Delta-HER2, has been shown to increase the anchorage-independent colony formation potential and tumorigenicity of rodent fibroblasts (6, 7). Delta-HER2 is the result of an in-frame deletion of exon 16 that produces a splice variant of HER2 lacking 16 amino acids in the juxtamembrane domain. This deletion causes an imbalance of cysteine residues and leads to the formation of disulphide-bridged homodimers and the constitutive activation of Delta-HER2 (7, 8). Interestingly, Delta-HER2 expression, which makes up approximately 2% to 9% of HER2 mRNA in human breast carcinomas (7, 9), correlates with the presence of lymph node metastases in human breast cancers and was suggested to confer resistance to trastuzumab in *in vitro* studies (10). Here, we describe the effects of Delta-HER2 in human breast epithelial cells. Overexpression of Delta-HER2, but not wild-type (WT)-HER2, increased and sustained proliferation, increased migration, and reduced apoptosis in MCF10A cells. It also led to the formation of invasive structures in three-dimensional (3D) cultures. Furthermore, unlike WT-HER2, overexpression of Delta-HER2 in human breast cells evoked mammary tumors

Authors' Affiliations: [1]Friedrich Miescher Institute for Biomedical Research (FMI); [2]Developmental and Molecular Pathways, Novartis Institutes for Biomedical Research, Basel, Switzerland

Note: Supplementary data for this article are available at Cancer Research Online (http://cancerres.aacrjournals.org/).

A. Alajati and N. Sausgruber contributed equally to this work.

Current address for A. Alajati: Institute of Oncology Research (IOR), Bellinzona, Switzerland and current address for N. Aceto: Massachusetts General Hospital Cancer Center, Harvard Medical School, Boston, Massachusetts.

Corresponding Authors: Mohamed Bentires-Alj, Friedrich Miescher Institute for Biomedical Research, Maulbeerstr. 66, Basel, CH 4058, Switzerland. Phone: 41-61-69-74048; Fax: 41-61-697-3976; E-mail: bentires@fmi.ch; and Abdullah Alajati, E-mail: abdullah.alajati@irb.unisi.ch

doi: 10.1158/0008-5472.CAN-12-3186

Published OnlineFirst July 18, 2013; DOI: 10.1158/0008-5472.CAN-12-3186

and lung metastases when injected into the mammary gland of immunodeficient mice. We have used proteomics and genomics approaches to identify changes in the phosphotyrosine proteome and in the transcriptome downstream of Delta-HER2. Together, the results presented increase our understanding of the activity of this tumorigenic splice variant of HER2 and reveal potential novel targets for HER2-positive breast cancer therapy.

Materials and Methods

Cell culture and constructs

Breast cancer cell lines BT474, SKBr3, ZR7530, T47D, HCC1965, MDA-MB-361, MDA-MB-231, MCF7, and ZR75.1 were grown as monolayer cultures as recommended by American Type Culture Collection. Primary human mammary epithelial cells MP5, MP8, and MP9 were prepared from reduction mammoplasty tissue obtained with appropriate informed consent and cultured as described previously (11). The immortalized but nontransformed MCF10A cells were grown and stained (12) as described previously. Briefly, in monolayer cultures, MCF10A cells were cultured in Dulbecco's Modified Eagle Medium (DMEM)/F12 medium (Invitrogen) supplemented with 5% horse serum (Hyclone), 20 ng/mL EGF (Peprotech), 0.5 μg/mL hydrocortisone (Sigma), 100 ng/mL cholera toxin (Sigma), 10 μg/mL insulin (Sigma), 100 IU/mL penicillin, and 100 μg/mL streptomycin. For 3D cultures, DMEM/F12 medium was supplemented with 2% horse serum, 5 ng/mL EGF, 0.5 μg/mL hydrocortisone, 100 ng/mL cholera toxin, 10 μg/mL insulin, 100 IU/mL penicillin, and 100 μg/mL streptomycin. To distinguish between specific effects of Delta-HER2 and signals emanating from growth factors in the medium, the cells were grown in DMEM/F12 medium supplemented with 100 IU/mL penicillin and 100 μg/mL streptomycin. WT-HER2 and Delta-HER2 were cloned into the pSD69 vector (11).

RNA isolation, cDNA synthesis, and primer sequences

RNA was extracted with TRIzol reagent (Sigma) and cDNA synthesized using ThermoScript RT-PCR System (Invitrogen) according to the manufacturer's instructions. The following primers were used for SYBR green-based quantitative real-time PCR (qRT-PCR): WT-HER2 forward 5′-CTGCACCCACTCCTGTGTGGACCTG-3′ and reverse 5′-CTGCCGTCGCTTGATGAGGATC-3′; Delta-HER2 forward 5′-CTGCACCCACTCCCCTCTGAC-3′ and reverse 5′-CTGCCGTCGCTTGATGAGGATC-3′, and GAPDH forward 5′-GAAGGTGAAGGTCGGAGTC-3′ and reverse 5′-GAAGATGGTGATGGGATTTC-3′.

Primer validation and quantitative real-time PCR

The efficiencies of primer pairs for WT-HER2, Delta-HER2, and glyceraldehyde-3-phosphate dehydrogenase (GAPDH) were calculated from C_t values obtained from serial 10-fold dilutions by linear regression of the log dilution factor versus the C_t values. The resulting primer pair efficiency was obtained from the slope of the regression line using the formula $E = 10^{(-1/\text{slope})}$; ref. 13); efficiencies were close to 2 for all primer pairs used. The specificities of the WT-HER2 primer pair for WT-HER2 and the Delta-HER2 primer pair for the splice variant Delta-HER2 were tested using MCF10A and MCF7 cell lines expressing either WT-HER2 or Delta-HER2, respectively. The ratios of WT-HER2 and Delta-HER2 expression in human breast tumors were calculated from $T_{Delta-HER2}/T_{WT-HER2} = (E_{WT-HER2})^{C_t\,WT-HER2}/(E_{Delta-HER2})^{C_t\,Delta-HER2}$, where T is the amount of mRNA, E is the primer efficiency, and C_t is the threshold cycle, as previously described (9, 13).

Human tumor samples

We obtained RNA samples of 8 human primary breast tumors from Origene. Tumors 1 to 4 (CR562849, CR560615, CR560630, and CR560397) were HER2-amplified and tumors 5 to 8 (CR562432, CR559736, CR560329, and CR561507) were HER2-positive.

Immunoblotting and antibodies

Total protein lysates for immunoblotting were obtained using L-buffer (2.5% SDS, 250 mmol/L Tris-HCl pH 7.4). The following antibodies were used: anti-HER2 (Calbiochem), anti-pHER2 (Tyr1248, Millipore), anti-AKT pan (Cell Signaling), anti-pAKT (Ser473, Cell Signaling), anti-ERK2 (Santa Cruz), anti-p-ERK1/2 (Thr202/Tyr204, Cell Signaling), anti-N-cadherin, anti-E-cadherin (BD Biosciences), and anti-K8 (Fitzgerald).

FACS analysis

MCF10A cells were dissociated with HyQTase (HyClone) and stained with Annexin V antibodies (Invitrogen) according to the manufacturers' protocols or with propidium iodide (Sigma). After staining, cells were analyzed by flow cytometry.

Transwell migration assays

Migration assays were conducted using Transwell chambers (8 μm pore size, BD Biosciences) according to the manufacturer's protocol. Briefly, starved cells were seeded in the top chamber at a concentration of 25,000 cells in 500 μL medium and 750 μL full growth medium was added to the bottom chamber. The cells were incubated for 24 hours at 37°C in 5% CO_2. Cells remaining in the top chamber were removed using a cotton swab and cells on the bottom surface of the membrane were fixed with 4% paraformaldehyde, stained with 0.2% crystal violet, and imaged using a Leica MacroFluo microscope.

Animal experiments

Experiments with SCID-beige mice (Jackson Labs) were carried out according to Swiss National guidelines on animal welfare. For orthotropic injection, 0.5 to 1×10^6 MCF10A cells or 1×10^6 MCF7 cells expressing WT-HER2 or Delta-HER2 were suspended in 100 μL of a 1:1 mixture of Basement Membrane Matrix Phenol Red-free (BD Biosciences) and PBS and injected into the mammary gland. For intravenous studies, MCF10A-Delta-HER2 cells were suspended in 50 μL PBS and injected into the tail vein. Trastuzumab (10 mg/kg) was administered intraperitoneally 3 times per week as described previously (14).

Immunohistochemistry

Staining of tumor and lung tissues was conducted automatically in a DiscoveryXT instrument (Ventana Medical Systems)

Published OnlineFirst July 18, 2013; DOI: 10.1158/0008-5472.CAN-12-3186

using the Research IHC DAB MapXT procedure. Paraffin was melted at 70°C for 30 minutes followed by 10 minutes at room temperature. Slides were incubated for 1 hour at 37°C after a mild CC1 pretreatment and manual application of HER2 antibody (Dako) at a dilution of 1/50. A biotinylated donkey anti-rabbit secondary antibody (Jackson Laboratories) was applied automatically followed by incubation for 32 minutes at 37°C. Sections were counterstained with Hematoxylin II and Bluing Reagent (Ventana Medical System), dehydrated, and mounted in Neo Mount (Merck).

Phosphotyrosine peptide profiling

Peptides containing pTyr residues were purified from trypsinized cell lysates using a two-step procedure and analyzed by liquid chromatography/tandem mass spectrometry (LC/MS-MS)(LTQ OrbiTrap XL, Thermo) as described (15). For relative quantification, duplicate runs for each sample were analyzed using Progenesis LCMS (Nonlinear Dynamics). All data are expressed as log2 ratios (Delta-HER2/WT-HER2). Database searches were conducted with Mascot Server using the human IPI database (version 3.64). Mass tolerances were set at 10 ppm for full MS scans and at 0.8 Da for MS-MS. Peptide identifications with a Mascot score of more than 20 were accepted. In cases of ambiguous assignment, spectra were interpreted manually to confirm the identity and localization of phosphorylation sites.

Microarray analysis

Total RNA was extracted from tumors with TRIzol reagent (Invitrogen), processed with a GeneChip WT cDNA Synthesis Kit and a GeneChip WT Terminal Labeling Kit (Affymetrix), hybridized for 16 hours to GeneChip Human Gene 1.0 ST arrays (Affymetrix), washed and scanned on a GeneChip Scanner 3000 with an autoloader according to the manufacturer's instructions. Expression values were normalized and probeset-level values calculated with robust multiarray average as implemented in the R/Bioconductor package affy (R version 2.14). Contrasts between MCF10A-Delta-HER2 and the other groups were computed with LIMMA (R/Bioconductor package). The data were filtered for a log-fold change LogFC > 2 between MCF10A-Delta-HER2 and MCF10-WT-HER2 to retrieve the "Delta-HER2 signature" (Supplementary Table S2) comprising 84 highly significant upregulated genes (adjusted $P < 3.54E{-}04$). CEL files have been deposited in the GEO repository (GSE42781). Unsupervised hierarchical clustering was conducted with Gene Cluster 3.0 (16). Expression values of annotated probe sets were filtered for a SD > 0.6 among the arrays. The resulting matrix containing 968 genes was mean centered and normalized. Uncentered correlation and centroid linkage were selected for the analysis. Java Treeview 1.1.6r2 (*Apristurus Saldanha*, Stanford, CA; ref. 5) was used to visualize the data. Gene set analysis (GSA) on primary breast tumors was conducted with the "gene expression-based outcome of breast cancer online" platform (10) as described previously (17). Association of the Delta-HER2 signature with clinical parameters was conducted on a merged dataset comprising 1,881 primary breast tumor samples obtained from multiple experiments. Distant metastasis-free survival for 10 years and 2 quantile analyses were conducted.

Results and Discussion

Expression of Delta-HER2 increases proliferation and migration of mammary cells

To address the effects of Delta-HER2 versus WT-HER2 signaling, we expressed human WT-HER2 or Delta-HER2 in the immortalized but nontransformed human breast epithelial cell line MCF10A and in the human breast cancer cell line MCF7 and compared expression to a panel of breast cancer cell lines (Supplementary Fig. S1A). The expression of Delta-HER2 in human breast tumors and cancer cell lines and in normal human breast cells was compared with the engineered MCF10A- and MCF7-Delta-HER2 cells. The efficiencies and specificities of primers designed to specifically detect either Delta-HER2 or WT-HER2 (Supplementary Fig. S1B) were validated in MCF10A and MCF7 cells expressing WT-HER2 or Delta-HER2 (Fig. 1A and Supplementary Fig. S1C). As expected, WT-HER2 was highly expressed in HER2-positive breast tumors and cancer cell lines but not in normal human breast cells. Notably, Delta-HER2 was expressed in all 8 primary HER2-positive human breast tumors and in some cell lines (Fig. 1A); the ratio of Delta-HER2 to WT-HER2 in tumors ranged from 0.7% to 3% (Supplementary Fig. S1D). Delta-HER2 expression in the engineered MCF10A- or MCF7-Delta-HER2 cells was comparable with or lower than that in the primary HER2-positive human breast tumors (Fig. 1A).

Overexpression of Delta-HER2 in MCF10A cells increased proliferation relative to the control or to the overexpression of WT-HER2 (Fig. 1B). Measurements of apoptosis by staining with anti-Annexin V antibodies and propidium iodide (PI) showed that the proportions of both Annexin V-positive and propidium iodide-positive cells were markedly lower in MCF10A-Delta-HER2 cells than in the controls (Fig. 1B). Thus, increased proliferation was accompanied by reduced cell death in MCF10A-Delta-HER2 cells.

Moreover, as shown by wound-healing and Transwell migration assays, overexpression of Delta-HER2 in MCF10A cells, but not of WT-HER2, increased their motility (Fig. 1C and Supplementary Fig. S1E). Interestingly, comparison of the phosphorylation status of several signaling molecules of the HER2 pathway in the absence of growth factors showed higher phosphorylation of HER2, ERK, and AKT in MCF10A-Delta-HER2 cells than in the MCF10A control or MCF10A-WT-HER2 cells (Fig. 1D).

To assess the effects of low-level expression of Delta-HER2, we generated MCF10A cells expressing Delta-HER2 or WT-HER2 (lines A, B, and C) at levels lower than MCF10A-Delta-HER2 or MCF10A-WT-HER2 (Fig. 1A and Supplementary Fig. S2A). Notably, low levels of Delta-HER2 but not of WT-HER2 increased the phosphorylation of ERK and AKT in starved cells (Supplementary Fig. S2A and S2B). Moreover, low-level expression of Delta-HER2 was sufficient to induce migration in Transwell migration assays (Supplementary Fig. S2D). Together these results indicate that expression of Delta-HER2 in MCF10A cells, but not of WT-HER2, at levels found in human tumors increases cell proliferation

Published OnlineFirst July 18, 2013; DOI: 10.1158/0008-5472.CAN-12-3186

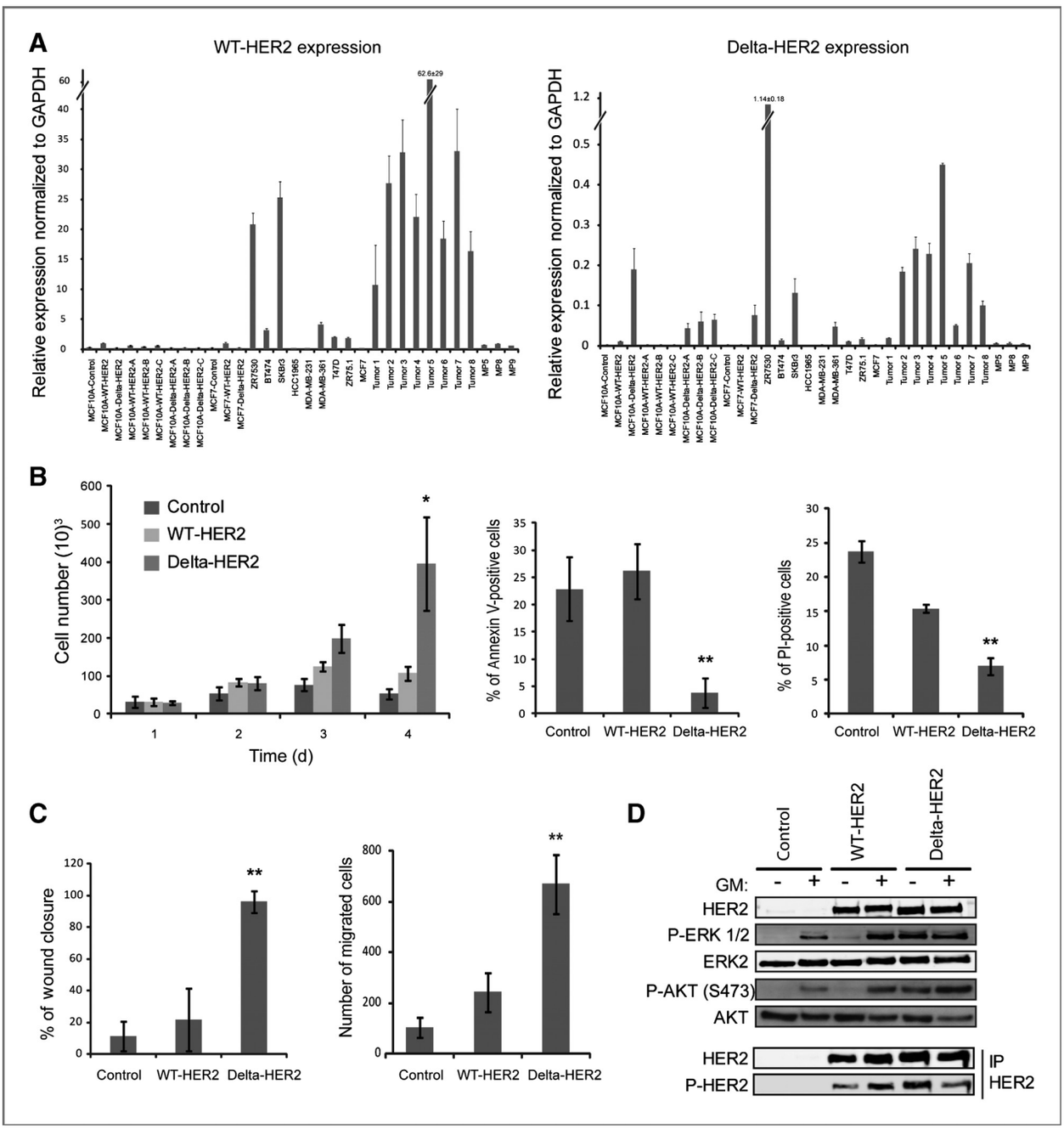

Figure 1. Delta-HER2 expression increases proliferation and migration but decreases apoptosis in mammary epithelial cells *in vitro*. A, qRT-PCR analysis of WT-HER2 and Delta-HER2 expression in breast cancer cell lines, human breast tumors (tumors 1–4 with HER2 amplification, tumors 5–8 HER2-positive), and in human breast epithelial cells isolated from reduction mammoplasties (MP5, MP8, and MP9). Results represent means ± SEM ($n = 3$–9). B, MCF10A cells were grown in starvation medium (DMEM/F12) for 1, 2, 3, or 4 days and the number of cells counted (left). The bar graph shows the absolute mean cell number (10^3) over time ± SD ($n = 6$; *, $P < 3.46E–06$). MCF10A cells expressing a control vector, WT-HER2, or Delta-HER2 were grown for 4 days in starvation medium and analyzed by flow cytometry for Annexin V expression (middle). The bar graph shows the mean percentage of Annexin V-positive cells ± SD ($n = 6$; **, $P < 0.000027$). MCF10A cells expressing a control vector, WT-HER2, or Delta-HER2 were grown for 2 days in starvation medium, stained with propidium iodide, and analyzed by flow cytometry (right). The bar graph shows the percentage of propidium iodide-positive cells ± SD ($n = 4$; **, $P < 2.6E–06$). C, wound-healing assay with MCF10A cells expressing a control vector, WT-HER2, or Delta-HER2 (left). The bar graph shows the mean percentage of wound closure ± SD ($n = 6$; **, $P < 5.16E–06$). Transwell assays with starved MCF10A cells expressing a control vector, WT-HER2, or Delta-HER2 (right). The bar graph shows the mean number of migrated cells ± SD ($n = 3$; *, $P < 0.05$). D, immunoblot of lysates from MFC10A cells expressing a control vector, WT-HER2, or Delta-HER2 (top). The cells were grown for 16 hours in the presence or absence of growth medium. Immunoprecipitation of HER2 followed by immunoblotting with the indicated antibodies (bottom).

Published OnlineFirst July 18, 2013; DOI: 10.1158/0008-5472.CAN-12-3186

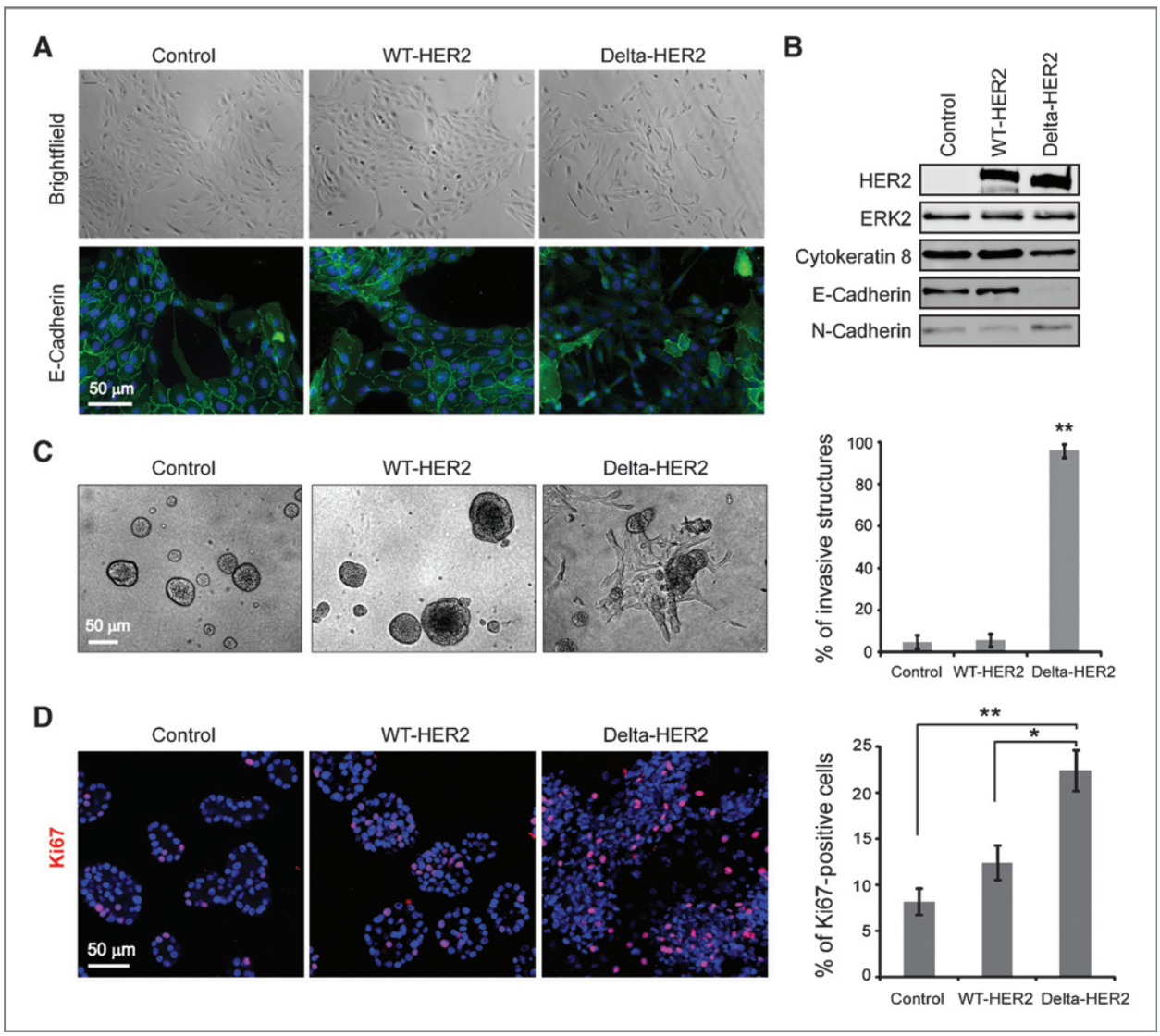

Figure 2. Delta-HER2 expression induces EMT and promotes invasion, proliferation, and loss of polarity in 3D cultures. A, top, representative phase-contrast images of MCF10A cells expressing a control vector, WT-HER2, or Delta-HER2 grown in monolayers. Immunostaining of E-cadherin (green) on MCF10A cells expressing a control vector, WT-HER2, or Delta-HER2 grown in monolayers (bottom). DAPI (blue) stained nuclei. B, immunoblot of lysates from MCF10A cells expressing a control vector, WT-HER2, or Delta-HER2 and grown in monolayers. C, representative phase-contrast images of MCF10A cells expressing a control vector, WT-HER2, or Delta-HER2 and grown in 3D cultures for 10 days (left). The bar graph shows the mean percentage of invasive structures $\pm$ SD ($n = 3$, **, $P < 4.2 \times 10^{-6}$; right). D, representative confocal images of equatorial cross-sections of MCF10 cells expressing a control vector, WT-HER2, or Delta-HER2 grown in 3D cultures for 15 days and stained for Ki67 (left). The bar graph shows the percentage of Ki67-positive cells (right). Results represent means $\pm$ SEM ($n = 4$; *, $P < 0.05$; **, $P < 0.005$).

and migration and decreases apoptosis; these effects were accompanied by constitutive activation of HER2, ERK, and AKT signaling.

Expression of Delta-HER2 induces epithelial-to-mesenchymal transition and invasion in 3D cultures

We examined whether expression of Delta-HER2 is associated with epithelial-to-mesenchymal (EMT) transition of MCF10A cells. To this end, we assessed the expression of E-cadherin, cytokeratin 8, and N-cadherin in MCF10A-WT-HER2 and MCF10A-Delta-HER2. Delta-HER2 expression in MCF10A cells was associated with downregulation of the epithelial markers cytokeratin 8 and E-cadherin and upregulation of the mesenchymal marker N-cadherin (Fig. 2A and B). Thus, unlike WT-HER2, Delta-HER2 expression resulted in EMT of MCF10A cells.

MCF10A control, MCF10A-WT-HER2, and MCF10A-Delta-HER2 cells were grown in 3D cultures for 10 days to assess invasion. Consistent with the migration and EMT results, Delta-HER2 expression caused the formation of highly invasive structures in 3D cultures (Fig. 2C). Staining for the proliferation marker Ki67 and the polarization markers laminin5 and

Published OnlineFirst July 18, 2013; DOI: 10.1158/0008-5472.CAN-12-3186

GM130 revealed an increase in the proportion of Ki67-positive cells in MCF10A-WT-HER2 and MCF10A-Delta-HER2 cultures compared with the control structures; there was no difference between structures expressing WT-HER2 or Delta-HER2 (Supplementary Fig. S3). Furthermore, after 10 days in 3D culture, the MCF10A control and WT-HER2 cells were polarized (the acinar structures displayed a basal expression of laminin5 and an apical expression of GM130), whereas the expression of Delta-HER2 impaired polarization (Supplementary Fig. S3). Staining MCF10A control, MCF10A-WT-HER2, and MCF10A-Delta-HER2 cells in 3D cultures for Ki67 after 15 days showed no difference in proliferation between control and MCF10A-WT-HER2 cells. In contrast, the expression of Delta-HER2 increased proliferation relative to the MCF10A control and WT-HER2 cells. Thus, Delta-HER2–induced proliferation, unlike WT-HER2, was a sustained effect present at both day 10 and 15 (Fig. 2D). Altogether, these data show that expression of Delta-HER2 sustains proliferation, mediates EMT, impairs polarization of mammary acinar structures, and induces invasion in 3D cultures.

Expression of Delta-HER2 induces tumor formation and metastasis

We examined whether the expression of Delta-HER2 in mammary epithelial cells is tumorigenic *per se*. To this end, we injected MCF10A or MCF7 cells expressing a control vector, WT-HER2 or Delta-HER2 (Supplementary Fig. S1A) into mammary glands of immunodeficient mice and assessed subsequent tumor development and growth. MCF10A-Delta HER2 but not MCF10A-WT-HER2 cells formed tumors when injected orthotopically into mice (Fig. 3A, left graph). The expression of Delta-HER2 in MCF7 cells increased MCF7 tumor growth, whereas WT-HER2 did not (Fig. 3A, right graph). Dissection of the lungs of MCF10A-Delta-HER2 tumor-bearing animals, followed by hematoxylin and eosin and HER2 immunohistochemical staining (Supplementary Fig. S4A), showed that 66% of mice-bearing MCF10A-Delta-HER2 tumors developed lung metastases (Fig. 3B). Furthermore, injection of MCF10A-Delta-HER2 cells into the tail vein of immunodeficient mice resulted in lung metastases in 71% of the animals (Fig. 3B). Thus, Delta-HER2 is tumorigenic and metastatic when expressed in MCF10A cells and also accelerated tumor onset and increased the tumor

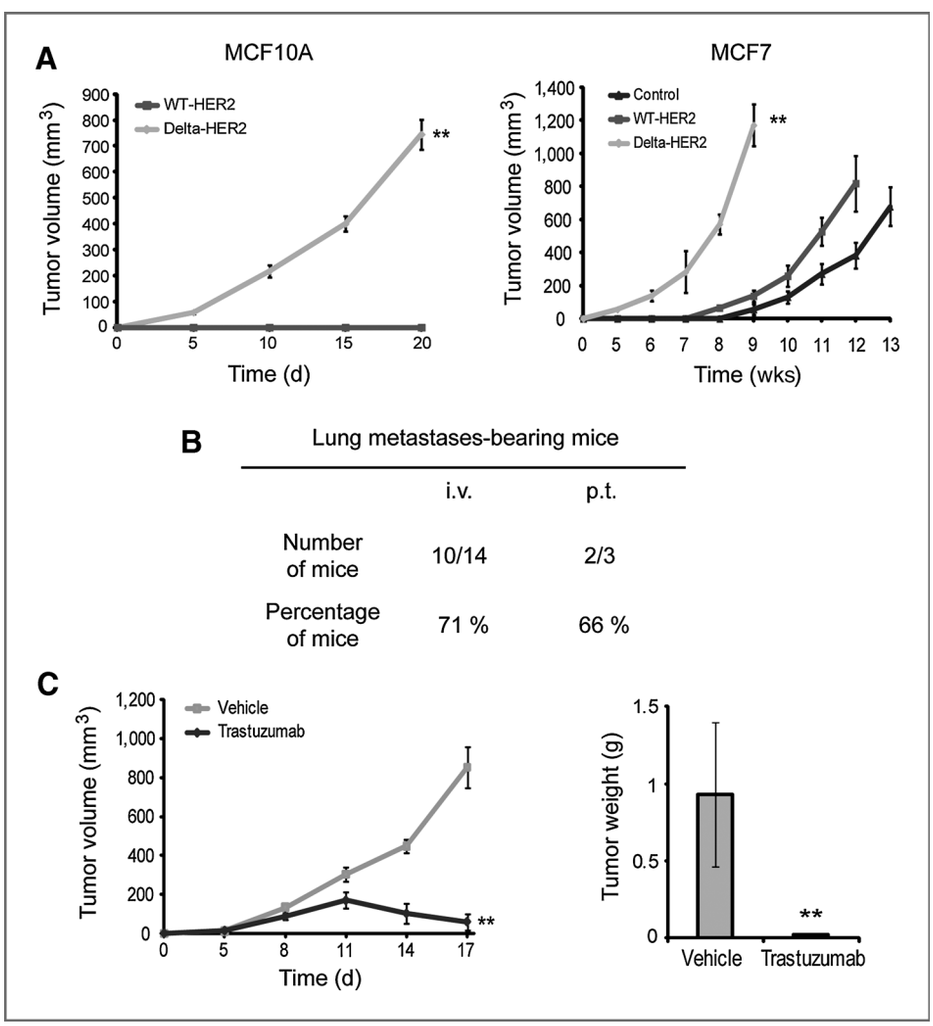

Figure 3. Overexpression of Delta-HER2 induces mammary tumors and lung metastases. A, tumor growth curves of MCF10A cells expressing WT-HER2 or Delta-HER2 showing mean tumor volumes (mm^3) ± SD ($n = 10$, **, $P < 1.8E–07$; left). Tumor growth curves of MCF7 cells expressing a control vector, WT-HER2, or Delta-HER2 showing the mean tumor volumes (mm^3) ± SD ($n = 6$, **, $P < 0.001$; right). B, table showing the numbers and percentages of mice that developed lung metastases after intravenous injection of MCF10A cells expressing Delta-HER2 or bearing a MCF10A-Delta-HER2 primary tumor (p.t). C, MCF10A-Delta-HER2 tumor-bearing mice were treated after tumors became palpable (7 days) with vehicle (PBS) or trastuzumab (10 mg/kg) 3 times per week. Tumor growth curves of MCF10A cells expressing Delta-HER2 and treated with vehicle or trastuzumab showing mean tumor volumes (mm^3) ± SD ($n = 9$, **, $P < 0.001$; left). Bar graph showing mean tumor weights (g) ± SD ($n = 9$, **, $P < 0.001$; right).

Published OnlineFirst July 18, 2013; DOI: 10.1158/0008-5472.CAN-12-3186

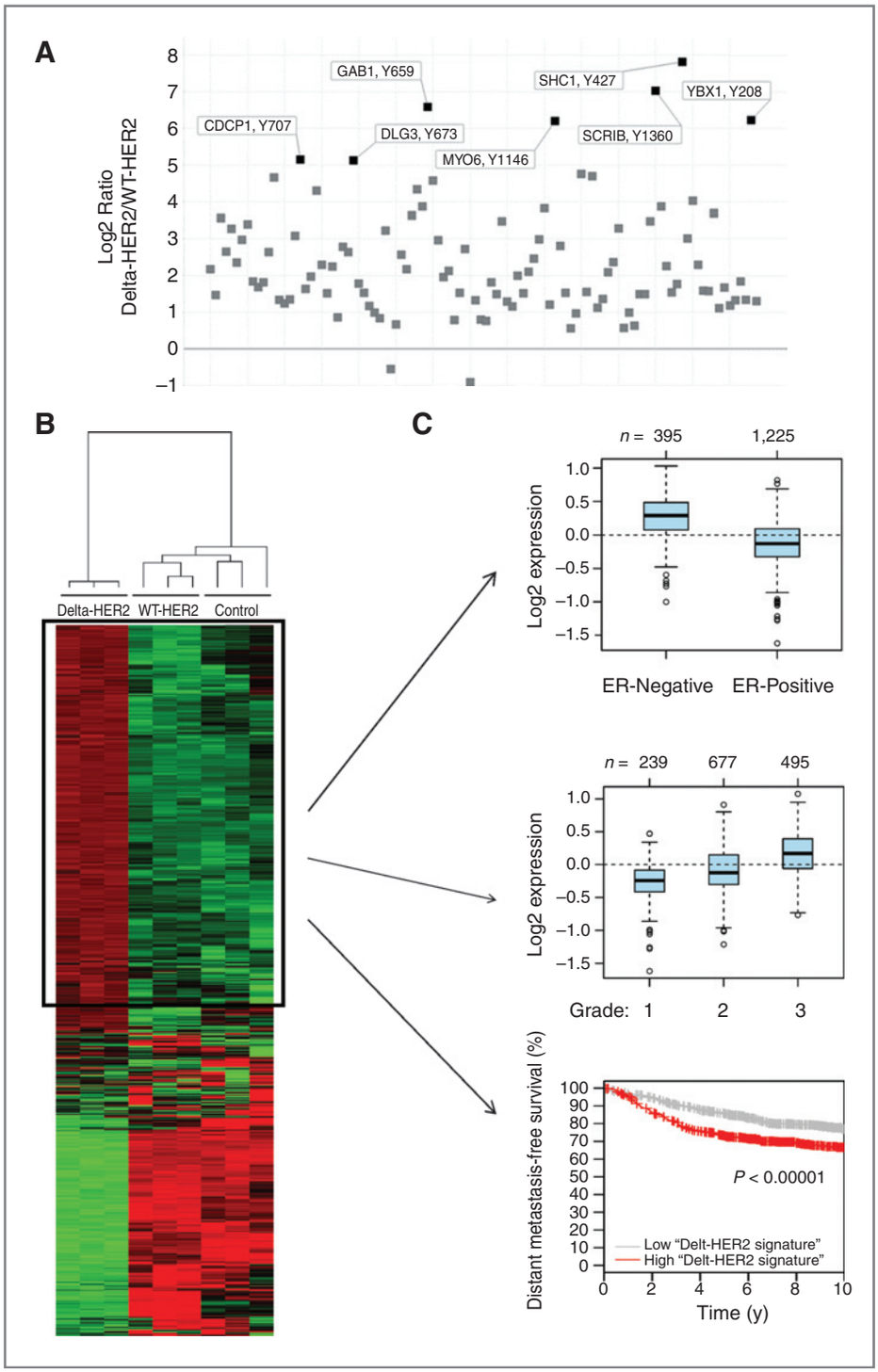

Figure 4. Effects of Delta-HER2 expression on the transcriptome and phosphotyrosine proteome. A, plot of the $\log_2$ ratios of Delta-HER2/WT-HER2 phosphopeptides identified by mass spectrometry. B, unsupervised hierarchical clustering of the microarray data obtained from MCF10A cells expressing a control vector, WT-HER2, or Delta-HER2. The rectangle highlights the genes specifically upregulated in MCF10A-Delta-HER2 cells and referred to as the Delta-HER2 signature. C, GSA of the Delta-HER2 signature genes in a dataset comprising 1,881 primary breast tumors (10). Top, box plot of Delta-HER2 signature gene expression in ER-negative and ER-positive primary breast cancers; $P < 0.0001$ by ANOVA. Middle, box plot of Delta-HER2 signature gene expression in grade 1, 2, and 3 primary breast cancers; $P < 0.0001$ by ANOVA. Numbers above the charts show the numbers of patients in each group. Bottom, Kaplan–Meier plot indicating the distant metastasis-free survival time of patients-bearing breast tumors with low or high expression of Delta-HER2 signature genes.

volume of MCF7 cells grown as xenografts. Consistent with the results *in vitro* (Supplementary Fig. S2A–S2C), low expression levels of Delta-HER2 in MCF10A evoked mammary tumors when injected into immunodeficient mice (Supplementary Fig. S2D).

Previous *in vitro* studies have reported that the HER2-targeting monoclonal antibody trastuzumab is ineffective when applied to Delta-HER2–expressing cells *in vitro* (10). Given the clinical importance of this observation, we asked whether this is also the case *in vivo*. MCF10A-Delta-HER2 cells were injected into immunodeficient mice and the mice treated with trastuzumab upon tumor development. In contrast with the previous *in vitro* findings (10), trastuzumab blocked tumor growth and proliferation (Fig. 3C and Supplementary Fig. S4B). These results show that the Delta-HER2–evoked tumors were

sensitive to trastuzumab *in vivo* and that they remained dependent on oncogenic signaling pathways emanating from the expression of this splice variant.

Delta-HER2 expression is associated with a distinct signaling cascade

To gain further insight into the signaling networks initiated by Delta-HER2 expression, we first compared protein–tyrosine phosphorylation events in MCF10A-WT-HER2 and MCF10A-Delta-HER2 cells using MS. This analysis revealed a distinct tyrosine-phosphorylation signature of MCF10A-Delta-HER2 cells, including increases in several known mediators of HER2 signaling (e.g., GAB1 and PTPN11) as well as the tyrosine phosphorylation of proteins not previously linked to the HER2 pathway (e.g., CDCP1; Fig. 4A and Supplementary Table S1). Moreover, microarray analysis of RNA extracts obtained from MCF10A cells expressing an empty vector, WT-HER2 or Delta-HER2 revealed a specific set of genes that were upregulated in MCF10A-Delta-HER2 cells (Fig. 4B and Supplementary Table S2). Most of these genes belong to the growth factor/cytokine family but also to cellular proliferation pathways (Supplementary Table S2). In an analysis of the Delta-HER2 signature genes in a breast cancer dataset (10, 17), their high expression correlated with clinicopathologic parameters such as estrogen receptor (ER)-negative status, high tumor grade, and poor distant metastasis-free survival (Fig. 4C).

Altogether, our data strongly suggest that the Delta-HER2 splice variant mediates proliferation, invasion, and tumorigenesis associated with metastatic spread when expressed in mammary cells. Analysis of the signaling cascade downstream of Delta-HER2 revealed increased tyrosine phosphorylation of several signaling molecules (some not previously linked to HER2 activation), as well as the expression of a Delta-HER2 signature associated with ER-negative status, high tumor grade, and metastasis in patients with breast cancer. These results may lead to the identification of novel therapeutic targets for treating Delta-HER2–positive breast cancers.

Disclosure of Potential Conflicts of Interest

No potential conflicts of interest were disclosed.

Authors' Contributions

Conception and design: A. Alajati, N. Sausgruber, N. Aceto, H. Voshol, M. Bentires-Alj

Development of methodology: A. Alajati, N. Aceto, S. Duss, H. Voshol

Acquisition of data (provided animals, acquired and managed patients, provided facilities, etc.): N. Sausgruber, N. Aceto, S. Sarre, H. Voshol, D. Bonenfant

Analysis and interpretation of data (e.g., statistical analysis, biostatistics, computational analysis): A. Alajati, N. Sausgruber, N. Aceto, S. Duss, H. Voshol, D. Bonenfant

Writing, review, and/or revision of the manuscript: A. Alajati, N. Sausgruber, N. Aceto, H. Voshol, M. Bentires-Alj

Administrative, technical, or material support (i.e., reporting or organizing data, constructing databases): A. Alajati, S. Duss, D. Bonenfant

Study supervision: M. Bentires-Alj

Acknowledgments

The authors thank Patrick Ringenbach, Sylvie Thiebault, and Veronique Lindner (Emile Muller, Centre Hospitalier de Mulhouse, Mulhouse, France) for providing mammary tissue, Gwen MacDonald (FMI) for technical assistance, Michael Stadler (FMI) for statistical analysis, and members of the Bentires-Alj lab for advice and discussions.

Grant Support

Research in the lab of M. Bentires-Alj is supported by the Novartis Research Foundation, the European Research Council (ERC starting grant 243211-PTPsBDC), the Swiss Cancer League, and the Krebsliga Beider Basel. N. Aceto is a fellow of the Swiss National Science Foundation. A. Alajati was supported by FP-7 Marie Curie fellowship.

The costs of publication of this article were defrayed in part by the payment of page charges. This article must therefore be hereby marked advertisement in accordance with 18 U.S.C. Section 1734 solely to indicate this fact.

Received August 14, 2012; revised May 13, 2013; accepted June 4, 2013; published OnlineFirst July 18, 2013.

References

1. Coughlin SS, Ekwueme DU. Breast cancer as a global health concern. Cancer Epidemiol 2009;33:315–8.
2. Hynes NE, MacDonald G. ErbB receptors and signaling pathways in cancer. Curr Opin Cell Biol 2009;21:177–84.
3. Nahta R, Esteva FJ. HER2 therapy: molecular mechanisms of trastuzumab resistance. Breast Cancer Res 2006;8:215.
4. Arribas J, Baselga J, Pedersen K, Parra-Palau JL. p95HER2 and breast cancer. Cancer Res 2011;71:1515–9.
5. Pedersen K, Angelini PD, Laos S, Bach-Faig A, Cunningham MP, Ferrer-Ramon C, et al. A naturally occurring HER2 carboxy-terminal fragment promotes mammary tumor growth and metastasis. Mol Cell Biol 2009;29:3319–31.
6. Kwong KY, Hung MC. A novel splice variant of HER2 with increased transformation activity. Mol Carcinog 1998;23:62–8.
7. Siegel PM, Ryan ED, Cardiff RD, Muller WJ. Elevated expression of activated forms of Neu/ErbB-2 and ErbB-3 are involved in the induction of mammary tumors in transgenic mice: implications for human breast cancer. EMBO J 1999;18:2149–64.
8. Ursini-Siegel J, Schade B, Cardiff RD, Muller WJ. Insights from transgenic mouse models of ERBB2-induced breast cancer. Nat Rev Cancer 2007;7:389–97.
9. Castiglioni F, Tagliabue E, Campiglio M, Pupa SM, Balsari A, Menard S. Role of exon-16-deleted HER2 in breast carcinomas. Endocr Relat Cancer 2006;13:221–32.
10. Mitra D, Brumlik MJ, Okamgba SU, Zhu Y, Duplessis TT, Parvani JG, et al. An oncogenic isoform of HER2 associated with locally disseminated breast cancer and trastuzumab resistance. Mol Cancer Ther 2009;8:2152–62.
11. Duss S, Andre S, Nicoulaz AL, Fiche M, Bonnefoi H, Brisken C, et al. An oestrogen-dependent model of breast cancer created by transformation of normal human mammary epithelial cells. Breast Cancer Res 2007;9:R38.
12. Aceto N, Sausgruber N, Brinkhaus H, Gaidatzis D, Martiny-Baron G, Mazzarol G, et al. Tyrosine phosphatase SHP2 promotes breast cancer progression and maintains tumor-initiating cells via activation of key transcription factors and a positive feedback signaling loop. Nat Med 2012;18:529–37.
13. Pfaffl MW. A new mathematical model for relative quantification in real-time RT-PCR. Nucleic Acids Res 2001;29:e45.
14. Zhao Y, Liu H, Liu Z, Ding Y, Ledoux SP, Wilson GL, et al. Overcoming trastuzumab resistance in breast cancer by targeting dysregulated glucose metabolism. Cancer Res 2011;71:4585–97.
15. Dey JH, Bianchi F, Voshol J, Bonenfant D, Oakeley EJ, Hynes NE. Targeting fibroblast growth factor receptors blocks PI3K/AKT signaling, induces apoptosis, and impairs mammary tumor outgrowth and metastasis. Cancer Res 2010;70:4151–62.
16. Eisen Lab: Software. Available from: http://rana.lbl.gov/EisenSoftware.htm.
17. Ringner M, Fredlund E, Hakkinen J, Borg A, Staaf J. GOBO: gene expression-based outcome for breast cancer online. PLoS ONE 2011;6:e17911.

Published OnlineFirst July 18, 2013; DOI: 10.1158/0008-5472.CAN-12-3186

Cancer Research
The Journal of Cancer Research (1916–1930) | The American Journal of Cancer (1931–1940)

AACR American Association for Cancer Research

Mammary Tumor Formation and Metastasis Evoked by a HER2 Splice Variant

Abdullah Alajati, Nina Sausgruber, Nicola Aceto, et al.

Cancer Res 2013;73:5320-5327. Published OnlineFirst July 18, 2013.